# Influence of piedmont sedimentation on erosion dynamics of an uplifting landscape: an experimental approach

Julien Babault, Stéphane Bonnet, Alain Crave, Jean van den Driessche

# Influence of piedmont sedimentation on erosion dynamics of an uplifting landscape: An experimental approach

**Julien Babault***

**Stéphane Bonnet**

**Alain Crave**

**Jean Van Den Driessche**

*Géosciences Rennes, Université de Rennes 1, UMR CNRS 6118, Campus de Beaulieu, 35042 Rennes cedex, France*

*Corresponding author e-mail: Julien.Babault@univ-rennes1.fr

**ABSTRACT**

Models of relief development generally assume that eroded products are evacuated far from the landscape whereas in nature they often deposit at the foot of mountain belts, within continental environments. Because piedmont aggradation can modify the base-level for erosion we ask what is the influence of piedmont sedimentation on the dynamics of an upstream relief. We developed an experimental study of relief dynamics using laboratory-scale models submitted to uplift under runoff-driven erosion. We compare the dynamics of topographies surrounded or not by a depositional belt made of eroded products coming from upstream. Piedmont aggradation acts on the dynamics of the upstream relief by modifying the relative uplift rate (applied uplift rate minus aggradation rate) that denudation tends to balance. Relief denudates at a lower rate than the applied uplift rate so the mean elevation of the uplifting topography rises. When the timescale of aggradation is higher than the timescale of relief development the topography cannot reach a steady-state between denudation and the applied uplift rate as long as aggradation occurs. However, in this case denudation balances a

continuously varying relative uplift rate during a dynamic equilibrium phase of the topography.

**Keywords**: relief dynamics, uplift, erosion, sedimentation, denudation, experimental modeling.

## INTRODUCTION

The relief of mountain belts results from the competing action of tectonic processes that create topography and of erosional processes that destroy it. Different models of relief dynamics have been proposed (Davis, 1889; Penck, 1953; Hack, 1960) following the timescale of these processes (Kooi and Beaumont, 1996). Among them, Hack (1960) argued that a steady state of the landscape may develop because of a balance between tectonic and erosional processes. The ability of a system to reach a steady-state depends on its response time with regard to variation in the external forcing parameters such as tectonics and climate (Kooi and Beaumont, 1996; Tucker and Slingerland, 1997; Whipple, 2001). The steady state of a relief submitted to a constant uplift rate implies constant macroscale geometry of the relief, then constant denudation rates and outward sediment flux.

Mountain ranges are usually bounded by sedimentary basins where eroded products accumulate. Sediment flux to basins depends on the erosional dynamics of the upstream reliefs and some works have tentatively used the sediment record as a proxy of relief dynamics (Pazzaglia and Brandon, 1996). Up to now, conceptual models of relief dynamics have been put forward independently of sedimentary processes within the basins. However, if sedimentation in front of a relief occurs above sea level (referred in the following as piedmont aggradation), it will modify its dynamics because it will act as an increase of the base-level for erosion, defined as the limit between erosion and sedimentation (Wheeler, 1964). The erosional dynamics of mountain belts will therefore be different depending on the nature of the surrounded sedimentary basins: underfilled or overfilled (e.g. Flemings and Jordan, 1989).

Moreover, as a foreland basin commonly evolves from underfilled to overfilled, changes in the base-level elevation has to control the denudation dynamics during mountain building. Here we investigate how sedimentation influence an upstream relief submitted to uplift by using an experimental approach of erosion dynamics.

## EXPERIMENTAL DESIGN AND PROCEDURE

We use an experimental device to simulate erosion of reliefs submitted to constant uplift and rainfall rates. The device is a modified version of a previous apparatus (Crave et al., 2000; Bonnet and Crave, 2003; Lague et al., 2003). The material eroded is a silica paste made of silica powder (D50 = 10μm) mixed with water. The silica paste fills a rectangular box (erosion box, size 400 × 600 mm and 500 mm deep) with a moveable base, upward or downward within the box. These movements are driven by a screw and a computer-controlled stepping motor. During an experiment, the base moves upward at a constant rate and pushes the silica paste outside the top of the erosion box at a rate defined as the uplift rate ($U$). The erosion box is located in a rainfall simulator where four industrial sprinklers deliver a high pressure water/air mixture. All experiments were run under the same rainfall rate of 120 ± 5 mm/h. During an experimental run, every 30 to 60 min, we stop the uplift and rainfall devices to construct 0.5 mm square-grid DEMs. Topographic information is derived from optical stereo data acquired with the Advanced TOpometric Sensor (ATOS) developed by the GOM Company.

We present results from three types of experiments (Table 1). Type 1 consists of four runs using different uplift rates. In these experiments the eroded products leave the erosion box (Fig. 1A). In type 2 the addition of a plateau surrounding the top of the erosion box allows the eroded products to deposit at the foot of the raising zone (Fig. 1B). Three experiments were run with the same uplift rate but with different sizes of surrounding plateau. The first phase of type 3 corresponds to type 1, followed by a second phase during which a

plateau is added as in type 2 in order to simulate a change in the basin depositional system stage (underfilled to overfilled) which is a striking characteristic of foreland basins evolution around mountain belts (e.g. Flemings and Jordan, 1989).

**RELIEF DYNAMICS WITHOUT PIEDMONT SEDIMENTATION (TYPE 1 EXPERIMENTS)**

When the experiments start, the top surface of the models is approximately flat. As uplift progresses topographic incisions develop along the four borders of the model and propagate inward until the complete dissection of the initial surface is achieved. Figure 2A shows the typical evolution of the mean elevation $<h>$ during such an experiment. During a first stage, the mean elevation progressively increases, corresponding to the growth phase of the landscape (Lague et al., 2003). In a second stage, the mean elevation stabilizes around a constant value. It defines a macroscale steady state of the relief (Hack, 1960) and implies that the output eroded flux equals the input uplift flux (Fig. 2A). Hereafter we characterize the experiments by using two parameters (Table1): $<h>_{s.s.}$, the mean elevation at steady state, and $\tau_{topo}$, the characteristic timescale to attain steady state. $\tau_{topo}$ is derived from an exponential fit of the mean elevation data during the growth phase, of the form:

$$< h >_{s.s.} = a + b(1 - e^{-t/\tau}) . \quad (1)$$

For four uplift rates we observe a positive threshold-linear relationship between $<h>_{s.s.}$ and $U$ (Fig. 3):

$$< h >_{s.s.} = < h_u > + \tau_u U , \quad (2)$$

with $<h_u>$ = 4.8 mm, and $\tau_u$ = 72 min. $\tau_{topo.}$ does not vary significantly with $U$ (Table 1) and is of the order of 94 min. The steady state occurs after around 300 min of erosion (Fig. 2A). The erosional behavior of the models and their dependency with $U$ are similar to those obtained by Lague et al. (2003).

## RELIEF DYNAMICS ASSOCIATED WITH PIEDMONT SEDIMENTATION (TYPE 2 EXPERIMENTS)

### Dynamics of sedimentation

Piedmont sedimentation of the eroded products does not change the sequence of the relief development with regard to the raising zone. At the outlet of the developing catchments small fans of sediments form that progressively coalesce into a unique larger one, as a natural bajada, surrounding the raising zone (Fig. 1B). As uplift and erosion progress, the fan progrades toward the plateau edge keeping its mean slope constant (~4°), whereas its apex elevation ($<h>_f$) increases (e.g. Fig. 2B). This dynamics lasts until the fan reaches the plateau edge where the particles can leave the system. Then no more aggradation occurs at the plateau edge whereas sediments still aggrade upslope. This results in a progressive increase of the fan slope up to a threshold slope (~6.5°), for which the whole fan becomes a by-pass zone. All the particles that are produced from now on by erosion within the raising zone leave the system so that $<h>_f$ no longer increases. The $<h>_f$ curve then shows a progressive decrease of the aggradation rate ($U_f$). Three experiments were performed that differ in the size of the deposition zone and hence in the time over which the fan becomes a by-pass zone ($\tau_f$, Table 1) and by the final elevation of the fan apexes ($<h>_{f\text{-}s.s}$, Table 1) (Figs. 2B, C and D). The greater the plateau, the longer the time before $<h>_f$ stabilizes (Fig. 4).

### Relief dynamics

Aggradation displaces upward the base level for the relief which then rises at a relative uplift rate ($U_r$) such that $U_r = U - U_f$. Stabilization of $<h>$ is never achieved as long as piedmont aggradation occurs (Fig. 2D), i.e. no steady state is defined according to the mean elevation criteria. As $U_r$ varies depending on a timescale defined by $\tau_f$, and as $<h>_{s.s}$ depends on the uplift rate (Fig. 3), the gradual change in $U_r$ prevents the development of any steady state. This is the case all along the experiment P1 (Fig. 2D). However, after 300 min the

denudation rate balances $U_r$ indicating that the subsequent topographies are at equilibrium (Fig. 2D). From that point onwards, denudation and the resulting topography adjust to a continuously changing uplift rate, that is, with imperceptible response time. Such behavior is defined as dynamic equilibrium (Hack, 1960). Note that the time necessary to reach dynamic equilibrium in experiment P1 is nearly the same as the time required for experiments without sedimentation to attain steady state. This suggests that the presence of a sedimentation zone does not influence the drainage network growth, nor the time required for erosion to balance a varying uplift rate (dynamic equilibrium).

By contrast with experiment P1, the fans stop aggrading in experiments P2 and P6. $U_r$ then approaches the uplift rate and a steady-state topography develops (Figs. 2B and C). In these experiments the timescale to reach steady state depends on $\tau_f$. During experiment P6 this time is roughly the same as $\tau_{topo}$ for experiments without piedmont sedimentation (Figs. 2A, B and Table 1), preventing any dynamic equilibrium.

In experiment P2, steady state is reached later than in experiments without sedimentation (450 min compared to 300 min: Figs. 2C and A), because $\tau_f$ here exceeds $\tau_{topo}$ (Table 1). Between 300 and 450 min the topography probably evolves under a state close to dynamic equilibrium. Indeed, although the denudation rate does not strictly equal $U_r$ (Fig. 2C), both show a similar evolution. For experiment P1, the steady state has not been reached because the required time was too long for the initial volume of silica paste used. As the deposition zone is extensive, $\tau_f$ greatly exceeds $\tau_{topo}$ (Table 1) and the dynamic equilibrium phase lasts a long time, at least 510 min.

For experiments with piedmont sedimentation that reached steady state (P2 and P6), $\langle h \rangle_{s.s.}$ lies far above the $\langle h \rangle_{s.s.}$ vs. $U$ trend defined by equation 2 (Fig. 3). The fan apex elevation being constant, a relative steady state mean elevation ($\langle h \rangle_{s.s.-r}$) can be defined, such that $\langle h \rangle_{s.s.-r} = \langle h \rangle_{s.s.} - \langle h \rangle_f$. When considering $\langle h \rangle_{s.s.-r}$, experiments P2 and P6 lie close to

the trend defined by equation 2. Similarly, the mean elevation of topographies at dynamic equilibrium ($<h>_{dyn.eq.}$) plotted against $U_r$ lies far above the trend defined by equation 2 (Fig. 3). However when considering the relative mean elevation at dynamic equilibrium, $<h>_{dyn.eq.-r} = <h>_{dyn.eq} - <h>_f$, it follows the trend defined by equation 2. Therefore, when denudation balances uplift the relationship between $<h>_{s.s.-r}$ and $U$, or between $<h>_{dyn.eq.-r}$ and $U_r$ is neither altered by the presence of a depositional zone nor by the nature of the equilibrium (steady state or dynamic equilibrium).

## RELIEF DYNAMICS PERTURBATION BY EMERGENT PIEDMONT AGGRADATION (TYPE 3 EXPERIMENT)

The first phase of the type 3 experiment corresponds to type 1 experiment (B6). As soon as a steady state is achieved, a plateau is added as in type 2 experiments (Fig. 2E). In this case the $<h>$ curve shows a two-stage evolution of the relief dynamics. The first stage (from 600 to 990 min) corresponds to the sudden increase of $<h>$ just after the addition of the plateau and consequently to the break of the previous steady state. The $<h>$ increase implies a decrease in the denudation rate. Topography dynamics during the second stage is similar to that of experiment P2, including a dynamic equilibrium phase. When the fan becomes a by-pass zone at 990 min, topography enters a new steady state, for which $<h>$ is much higher than for the previous steady state.

## DISCUSSION

A direct application to natural systems is not reliable as perfect scaling of laboratory-scale reliefs is nearly impossible (Crave et al., 2000; Hasbargen and Paola, 2000; Lague et al., 2003). However results from modeling can be used to emphasize general concepts of landscape behavior. The present experiments highlight the importance of the elevation dynamics of the piedmont at the catchment's outlets. The results from this study highlight that erosional dynamics are modified if the timescale of piedmont aggradation is higher than the

timescale of relief development. In this case, after a period of drainage network growth, the relief enters a period of dynamic equilibrium. The transition from dynamic equilibrium to steady state occurs only if aggradation stops. Piedmont aggradation can consequently impose its dynamics to a relief submitted to uplift (Fig. 4). Whatever the timescale of processes, the second main effect of piedmont deposition is to shift the elevation of the drainage basins upward because relief denudates at a lower rate than the uplift rate. This results in the increase of the absolute elevation of the whole topography by an amount equal to the mean elevation of the fan apex (Fig. 3), which defines the base level of the upraising relief. The linear relation between the uplift rate and the mean elevation, as observed in experiments without piedmont sedimentation, also applies between the relative uplift rate and the relative mean elevation for experiments with piedmont sedimentation (Fig. 3).

Finally, the results of these experiments suggest that in nature piedmont sedimentation may contribute to the very high elevation of mountain peaks that surround high plateaus (eg. Tibet, Altiplano) and that the transition from underfilled foreland basins to overfilled foreland basins will result in the lowering of the denudation rate of upraising mountain belts without involving any reduction of the tectonic uplift rate.

**ACKNOWLEDGEMENTS**

We are most grateful to Chris Paola and an anonymous reviewer in improving the paper. Special thanks to Jean-Jacques Kermarrec for his help in the development of the experimental apparatus. We thank Polo and Laure for the all night long duties during the experiments. Mimi Hill one more time kindly improved the English. Financial support was provided by CNRS-INSU research program PNSE and ATI. This study was also supported by the Ministère de l'Education Nationale, de la Recherche et de la Technologie, who funded Julien Babault's Ph.D. thesis.

**REFERENCES CITED**

Bonnet, S., and Crave, A., 2003, Landscape reponse to climate change: Insights from experimental modelling and implications for tectonic versus climatic uplift of topography: Geology, v. 31, p. 123-126.

Crave, A., Lague, D., Davy, P., Kermarrec, J., Sokoutis, S., Bodet, L., and Compagnon, R., 2000, Analogue Modelling of Relief Dynamics: Physics and Chemistry of the Earth, Part A: Solid Earth and Geodesy, v. 25, p. 549-553.

Davis, W.M., 1889, The geographical cycle: Geogr. J., v. 14, p. 481-504.

Flemings, P.B., and Jordan, T.E., 1989, A synthetic stratigraphic model of foreland basin development: Journal of Geophysical Research, v. 94(B4), p. 3851-3866.

Hack, J.T., 1960, Interpretation of erosional topography in humid temperate regions: American-Journal-of-Science, v. 258, p. 80– 97.

Hasbargen, L.E., and Paola, C., 2000, Landscape instability in an experimental drainage basin: Geology, v. 28, p. 1067-1070.

Kooi, H., and Beaumont, C., 1996, Large-scale geomorphology: Classical concepts reconciled and integrated with contemporary ideas via a surface processes model: Journal of Geophysical Research, v. 101, p. 3361-3386.

Lague, D., Crave, A., and Davy, P., 2003, Laboratory experiments simulating the geomorphic response to tectonic uplift: Journal-of-geophysical-research, v. 108, p. ETG3.1-ETG3.20; 2.

Pazzaglia, F.J., and Brandon, M.T., 1996, Macrogeomorphic evolution of the post-Triassic Appalachian mountains determined by deconvolution of the offshore basin sedimentary record: Basin Res., v. 8, p. 255-278.

Penck, W., 1953, Morphological analysis of landforms: London, Macmillan, 429 p.

Tucker, G.E., and Slingerland, R., 1997, Drainage basin responses to climate change: Water Resour. Res., v. 33, p. 2031-2047.

Wheeler, H.E., 1964, Baselevel, lithosphere surface and time-stratigraphy: Geol. Soc. Am. Bull., v. 75, p. 599-610.

Whipple, K.X., 2001, Fluvial landscape response time: How plausible is steady-state denudation: American-Journal-of-Science, v. 301, p. 313-325.

**FIGURE CAPTIONS**

Figure 1. A: Oblique view of experiment at steady state without piedmont deposition (type 1: experiment B6 at $t$ = 360 min). B: Oblique view of experiment at dynamic equilibrium associated with piedmont deposition (type 2: experiment P2 at $t$ = 380 min). Size $L$ of deposition zone is 250 mm.

Figure 2. Graphs showing mean elevation $<h>$ of topography and mean fan apex elevation $(<h>_f)$ evolutions of type 1 (A: B6), type 2 (B: P6; C: P2; D: P1), and type 3 (E: P5) experiments. Experiments evolved with the same uplift rate $(U)$ of 15 mm/h and rainfall rate of 120 mm/h (Table 1). Steady state is defined by constant mean elevation (cste) of relief through time and by denudation rate $(D)$ that equals uplift rate. Dynamic equilibrium (Dyn. Eq.) is defined when denudation rate equals relative uplift rate $(U_r)$. "Fan limit" refers to the time the fan reaches the plateau edge.

Figure 3. Absolute (cross and solid symbols) or relative (open symbols) steady state (s.s.) and dynamic equilibrium (dyn. eq.) mean elevations of continuously uplifted zone against absolute (steady-state topographies) or relative uplift rate (dynamic equilibrium topographies). Solid line shows fit of mean elevation of type 1 experiments at steady state against imposed uplift rate.

Figure 4. Mean value of characteristic timescale to attain steady state for type 1 experiments that evolved without piedmont deposition (solid circle) and characteristic timescale of deposition zone to attain stabilization of $<h>_f$ (open circle). Data are plotted against size of deposition zone. For plateau size larger than 125 mm, timescale of deposition zone is higher

than timescale of relief development. In this case, the deposition zone imprints its dynamics to the relief, which then evolved under dynamic equilibrium after a growth phase of the drainage network. Thick gray line indicates the general characteristic timescale for an uplifted zone to reach steady state whether surrounded by a deposit zone or not.

TABLE 1. EXPERIMENTAL CONDITIONS AND RESULTS

| Name | Uplift rate (mm/h) | Rainfall rate (mm/h) | Erosion box boundaries (mm) | $\langle h \rangle_{s.s.}$ (mm) | $\langle h \rangle_{s.s.-r}$ (mm) | $\langle h \rangle_{f\text{-}s.s.}$ (mm) | $\tau_{topo}$ (min) | $\tau_f$ (min) |
|---|---|---|---|---|---|---|---|---|
| Type 1 experiments | | | | | | | | |
| B4 | 5 | 120 | free | 11.3 | - | - | 95±07 | - |
| B1 | 10 | 120 | free | 18 | - | - | 93±06 | - |
| B6 | 15 | 120 | free | 19.5 | - | - | 98±07 | - |
| B3 | 20 | 120 | free | 31 | - | - | 89±06 | - |
| Type 2 experiments | | | | | | | | |
| P6 | 15 | 120 | plateau 125 | 33.4 | 19 | 14 | - | 107±10 |
| P2 | 15 | 120 | plateau 150 | 44.8 | 19.6 | 25 | - | 247±30 |
| P1 | 15 | 120 | plateau 500 | 55.8* | 18.2* | 52† | - | 513±40 |
| Type 3 experiments | | | | | | | | |
| P5 | 15 | 120 | plateau 250 | 47.8 | 21 | 27 | - | 140±08 |

*Note:* the $\tau_f$ is calculated from an exponential fit of the $\langle h \rangle_f$ curve as $\tau_{topo}$.

*$\langle h \rangle_{dyn.eq.}$ and $\langle h \rangle_{dyn.eq.-r}$ of dynamic equilibrium for $U_r = 13.6$ mm/h at $t = 810$ min.

†Estimated value from an exponential fit of the $\langle h \rangle_f$ curve.

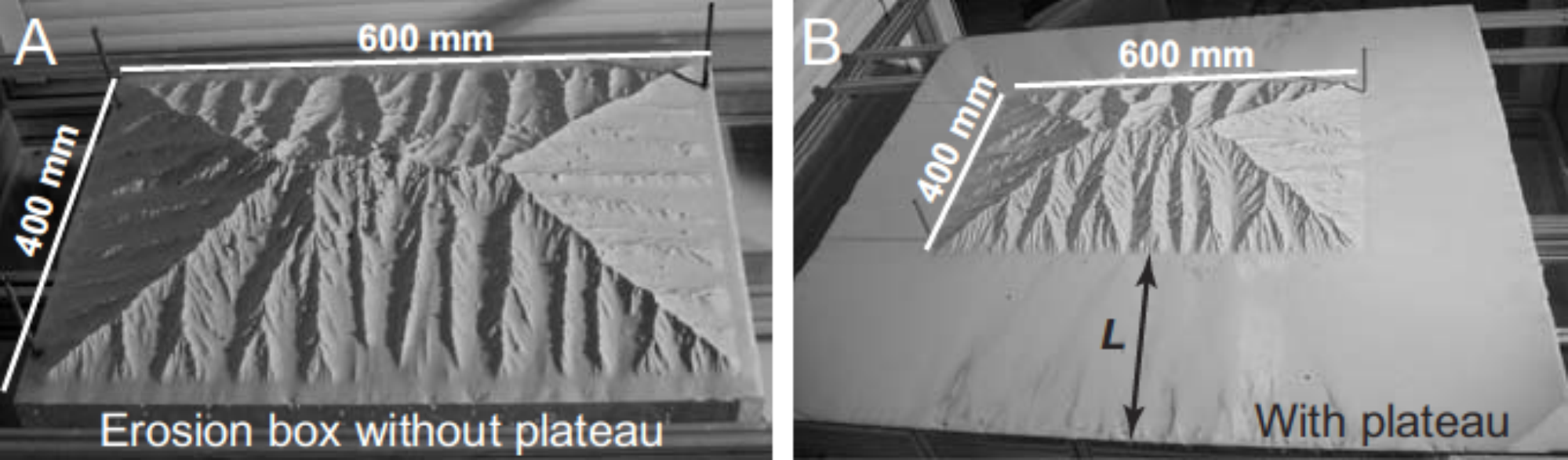
A
600 mm
400 mm
Erosion box without plateau
B
600 mm
400 mm
L
With plateau

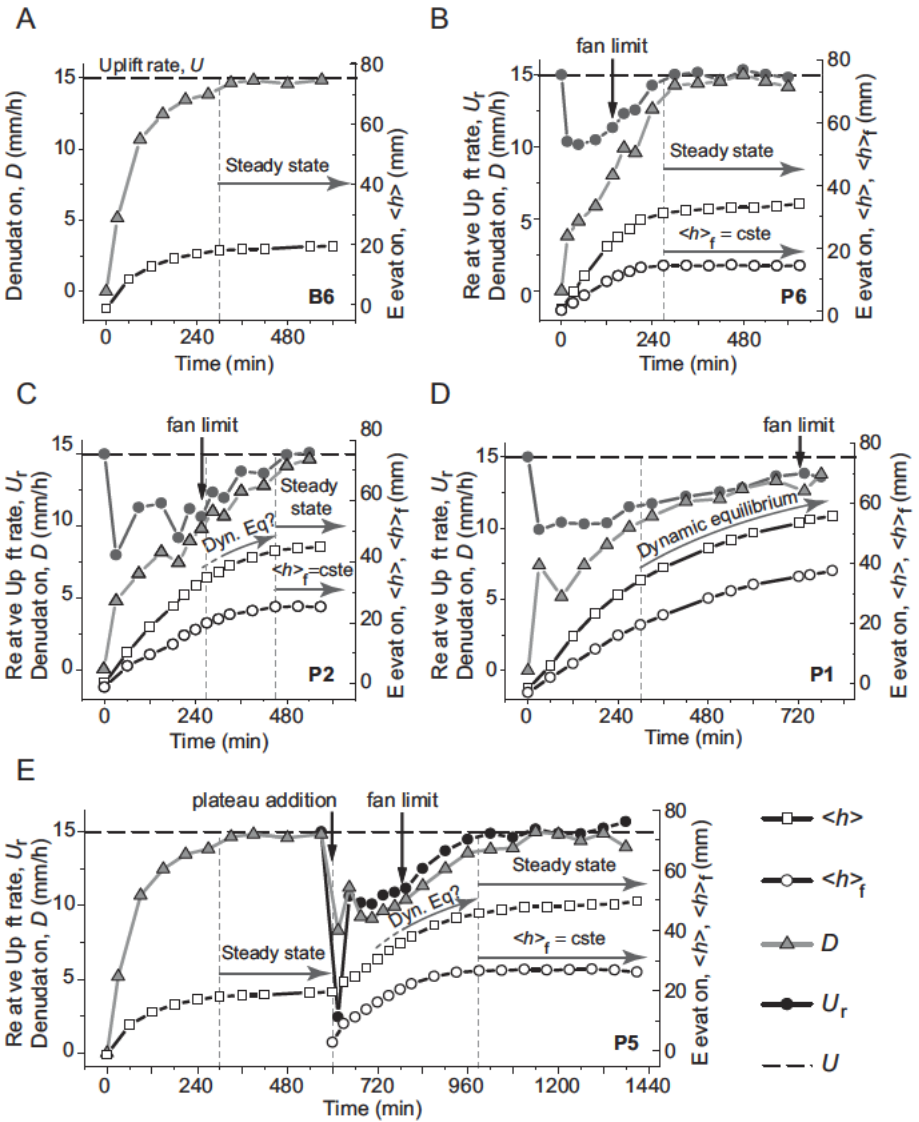
A
Uplift rate, U
Steady state
B6
Denudation, D (mm/h)
Erosion, <h> (mm)
Time (min)
B
fan limit
Steady state
<h>f = cste
P6
Reactive Uplift rate, Ur
Denudation, D (mm/h)
Erosion, <h>, <h>f (mm)
Time (min)
C
fan limit
Steady state
Dyn. Eq?
<h>f=cste
P2
Reactive Uplift rate, Ur
Denudation, D (mm/h)
Erosion, <h>, <h>f (mm)
Time (min)
D
fan limit
Dynamic equilibrium
P1
Reactive Uplift rate, Ur
Denudation, D (mm/h)
Erosion, <h>, <h>f (mm)
Time (min)
E
plateau addition
fan limit
Steady state
Steady state
Dyn. Eq?
<h>f = cste
P5
Reactive Uplift rate, Ur
Denudation, D (mm/h)
Erosion, <h>, <h>f (mm)
Time (min)
<h>
<h>f
D
Ur
U

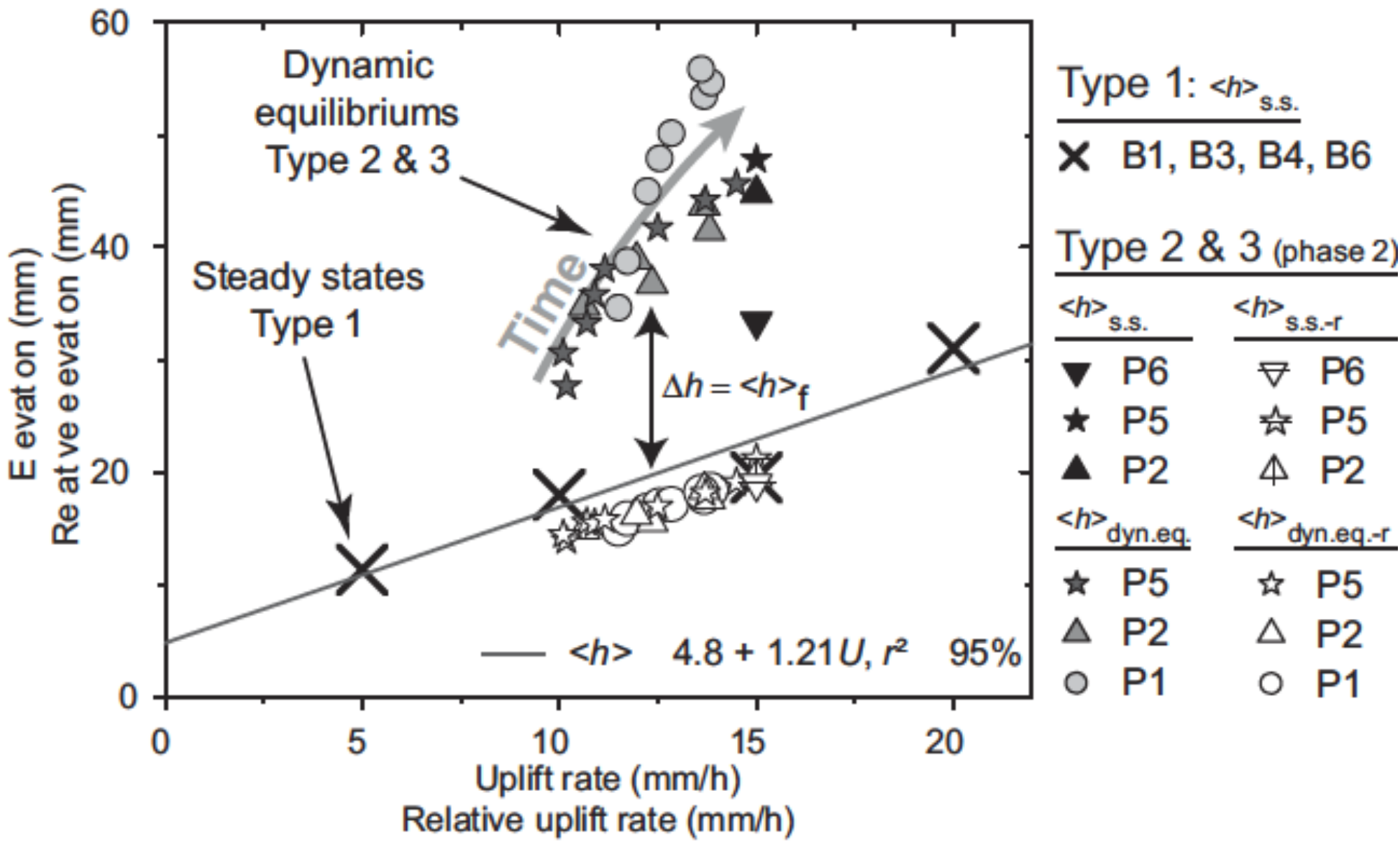
Dynamic equilibriums Type 2 & 3
Steady states Type 1
Time
Δh = <h>f
— <h> 4.8 + 1.21U, r² 95%
E evat on (mm)
Re at ve e evat on (mm)
Uplift rate (mm/h)
Relative uplift rate (mm/h)
0
20
40
60
0
5
10
15
20
Type 1: <h>s.s.
B1, B3, B4, B6
Type 2 & 3 (phase 2)
<h>s.s.
P6
P5
P2
<h>s.s.-r
P6
P5
P2
<h>dyn.eq.
P5
P2
P1
<h>dyn.eq.-r
P5
P2
P1

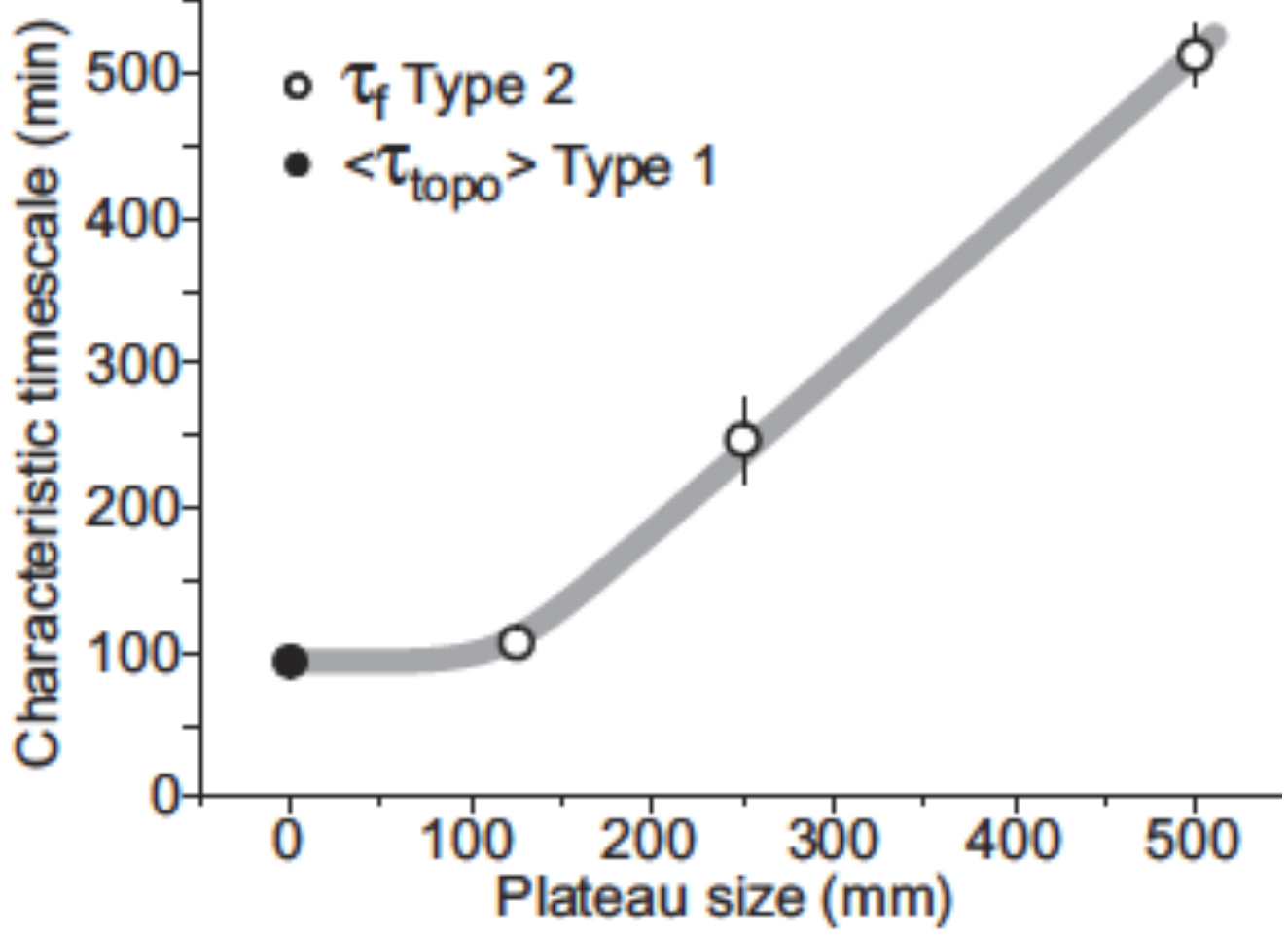
Characteristic timescale (min)
0
100
200
300
400
500
τf Type 2
<τtopo> Type 1
0
100
200
300
400
500
Plateau size (mm)